SPHERICAL EQUIVALENCY OF CYLINDRICAL CHARGES IN FREE-AIR

by

Edward D. Esparza
Southwest Research Institute
San Antonio, Texas

25th Department of Defense Explosives Safety Seminar
18-20 August 1992

ABSTRACT

Few experimental investigations can be found in the literature in which free-air blast parameters from cylindrical charges have been measured. As part of the work to update the DOE/TIC Manual 11268, "Prediction of Blast and Fragment Loadings on Structures," these free-air blast data were reviewed and analyzed. One of these sets of experimental data was used to develop graphs of equivalent spherical weights for cylindrical charges with length-to-diameter ratios of 1/4, 1/1, and 4/1. The actual peak side-on overpressure and impulse data from Pentolite cylindrical charges initiated at one end were scaled to standard sea level conditions using Sachs' scaling factors and the charge weights converted to equivalent TNT values based on Pentolite spherical charge test data. Then, equivalent spherical weights were determined using the standard air blast curves for spherical TNT detonations in free-air. Side-on pressure and impulse data measured along eight radials at 22.5° increments and at scaled distances of about 3 to 15ft/lb$^{1/3}$ were used to develop the equivalent spherical mass ratios. These results show the significant difference a cylindrical charge geometry has on the free-air blast loads as compared to spherical charges. To demonstrate further this difference, impulse amplitude ratios for one cylindrical charge versus a spherical charge were computed and applied to the reflected impulse loads on a flat surface from a free-air burst.

Report Documentation Page

Form Approved
OMB No. 0704-0188

1. REPORT DATE **AUG 1992**	2. REPORT TYPE	3. DATES COVERED **00-00-1992 to 00-00-1992**

4. TITLE AND SUBTITLE **Spherical Equivalency of Cylindrical Charges in Free-Air**	5a. CONTRACT NUMBER 5b. GRANT NUMBER 5c. PROGRAM ELEMENT NUMBER
6. AUTHOR(S)	5d. PROJECT NUMBER 5e. TASK NUMBER 5f. WORK UNIT NUMBER
7. PERFORMING ORGANIZATION NAME(S) AND ADDRESS(ES) **Southwest Research Institute,6220 Culebra Road,San Antonio,TX,78238-5166**	8. PERFORMING ORGANIZATION REPORT NUMBER
9. SPONSORING/MONITORING AGENCY NAME(S) AND ADDRESS(ES)	10. SPONSOR/MONITOR'S ACRONYM(S) 11. SPONSOR/MONITOR'S REPORT NUMBER(S)

12. DISTRIBUTION/AVAILABILITY STATEMENT
Approved for public release; distribution unlimited

13. SUPPLEMENTARY NOTES
See also ADA260984, Volume I. Minutes of the Twenty-Fifth Explosives Safety Seminar Held in Anaheim, CA on 18-20 August 1992.

14. ABSTRACT
see report

15. SUBJECT TERMS

16. SECURITY CLASSIFICATION OF:			17. LIMITATION OF ABSTRACT	18. NUMBER OF PAGES	19a. NAME OF RESPONSIBLE PERSON
a. REPORT **unclassified**	b. ABSTRACT **unclassified**	c. THIS PAGE **unclassified**	**Same as Report (SAR)**	**26**	

Standard Form 298 (Rev. 8-98)
Prescribed by ANSI Std Z39-18

INTRODUCTION

A considerable volume of data can be found in the literature which characterize the air blast wave generated by a spherical high explosive charge detonated in free-air. For example, Goodman[1] compiled a large number of free-air measurements from spherical Pentolite experiments dating from World War II to 1960. Using these data, Goodman [1] developed a set of "standard" curves for Pentolite. Baker [2] provides an excellent historical summary of free-air measurements up to 1970. He also developed a set of standard curves for spherical charges using energy as the scaling parameter making them directly applicable to any high explosive. In 1984, Kingery and Bulmash[3] compiled experimental and computational data for TNT and Pentolite to develop an updated set of scaled standard curves for TNT spherical charges in free-air and TNT hemispherical charges on the ground. These updated curves were developed to revise the TNT standard curves in the triservice manual, Structures to Resist the Effects of Accidental Explosions [4]. Revision 1 of this manual [5] includes these curves. To apply these curves to spherical charges of explosives other than TNT, TNT equivalent weights are used.

For non-spherical free-air denotations fewer experimental studies can be found reported in the literature. For a non-spherical charge, the shock wave will not enter the surrounding air as a spherical wave, nor at the same instant over the entire charge surface. The shape and strength of the shock wave entering the air will depend both upon charge geometry, and upon the relative location at which initiation occurred. The blast parameters will be functions not only of radial standoff, but also of azimuth and possibly elevation. Several experimental programs, such as those reported in References 6 through 14, investigated the blast field around non-spherical explosives of regular geometries such as cylinders, cubes, or cones. In many instances the charges were detonated in free-air, but measurements are sometimes only of reflected parameters and along one axis.

As part of the work to update DOE/TIC Manual 11268 [15], data found in the literature from cylindrical charges were reviewed and analyzed. In Reference 15, the results of an analysis by Plooster[16] of free-air side-on pressures calculated from time-of-arrival measurements made by Wisotski and Snyer[17] and by Parks and Weeding[18] were used as a method to estimate side-on pressures from free-air cylindrical charges of three aspect ratios for a limited range of scaled distances. The results presented in Reference 16 are multi-parameter curve fits which relate the peak side-on pressure P_s to the scaled distance Z, to the length-to-diameter ratio L/D, and to the azimuth angle θ (the angle between the longitudinal axis of the cylinder and the measurement axis). These were modified slightly in Reference 15 to make them applicable to TNT charges at sea level conditions.

In the recent work at Southwest Research Institute (SwRI) to revise Reference 15, direct measurements of side-on pressure and impulse from a more recent test program of cylindrical charges conducted by Plooster[19] were found in the literature search. Reference 19 reports on the experimental measurements made from end-initiated cylindrical charges detonated in free-air. These more recent data were analyzed by SwRI to develop equivalent spherical weights for cylindrical charges with L/D of 1/4, 1/1, and 4/1. The results were included in DOE/TIC Manual 11268, Revision 1[20]. This paper will present these results as well as some of the results of additional analysis to develop pressure and impulse amplitude ratio curve fits for certain azimuth angles from a cylindrical charge with an aspect ratio of 4/1.

ANALYSIS OF CYLINDRICAL DATA

In the test program described in Reference 19, experiments were conducted with end-initiated cylindrical Pentolite charges. Pressure-time recordings were made along radials at 22.5° increments as shown in Figure 1 and at several standoff distances. Most of the tests used cast Pentolite, 8 lb cylindrical charges with a few 16 lb charges also being fired. Some tests using 8 lb Pentolite spheres were fired throughout the program for internal calibration purposes. The test arena was laid out with two radial lines of side-on pressure transducers (6 sensors per line) placed 90° apart. Thus, each test generated pressure-time histories at two angles. The cylindrical charges were fired with their axes horizontal as indicated in Figure 1 and 12 ft above the ground to minimize ground reflections from interfering with the initial blast wave at the transducer locations. The pencil gages were also mounted at an elevation of 12 ft and at radial distances ranging from 7 to 31 ft. To obtain data at 22.5° intervals, the cylindrical charge was rotated relative to the two orthogonal transducer radials from test to test. Thus, data were obtained at each angle of interest in 5 tests.

Pentolite cylindrical charges of seven L/D ratios were used. However, measurements were made at all nine of the 22.5° intervals and in multiple firings only for charges with L/D ratios of 1/4, 1/1, and 4/1. Consequently, the analyses performed in rewriting Reference 15, and in writing this paper, used data only from tests using these 3 aspect ratios. Tabulations of the peak pressure P_s and positive impulse i_s data as measured at an average ambient pressure of 11.9 psia are presented in Reference 19. These data are also plotted in that reference scaled to a charge weight of one pound and to sea-level ambient pressure as a function of L/D for different scaled distances for a particular azimuth angle θ, and as a function of θ for different scaled distances for a particular L/D. Note that since cylindrical charges often generate secondary shock waves which are comparable or of greater amplitude than the leading shock, the pressure data tabulated in Reference 19 include any such significant peak pressures.

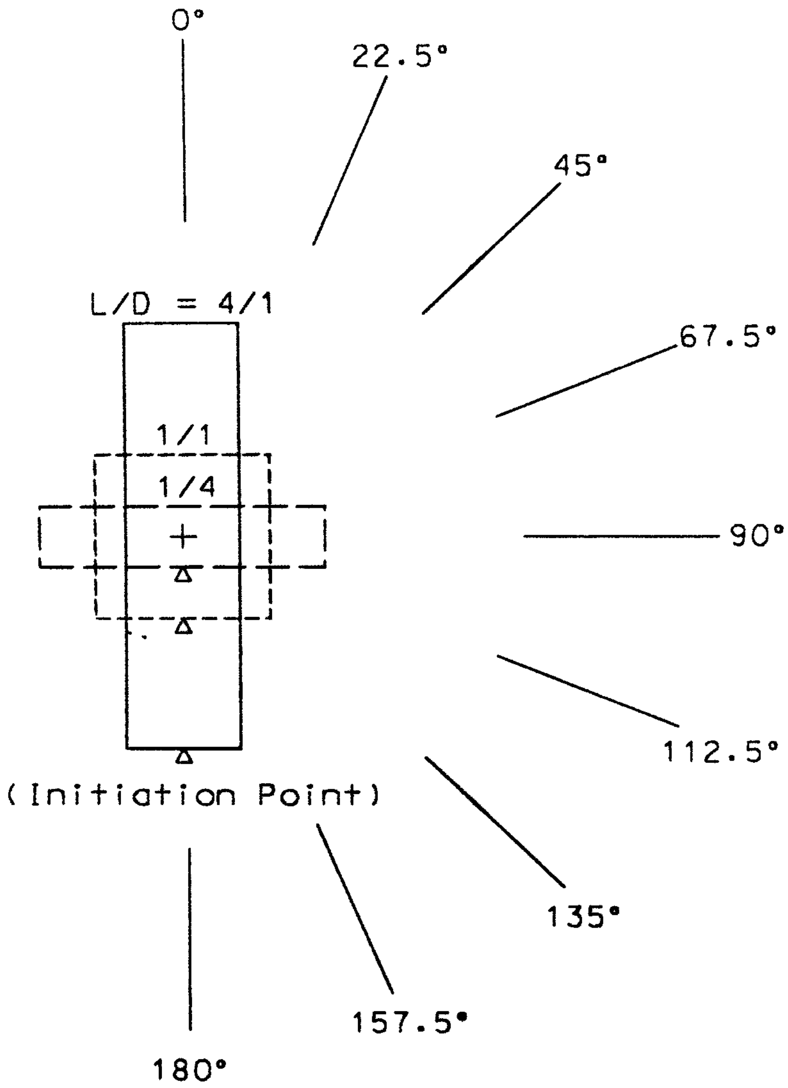

Figure 1. Plan View of Measurement Lines for a Free-Air Cylindrical Charge

To provide structural designers using Reference 20 with at least approximate correction factors to account for cylindrical charge geometry in determining blast loads, the data from Reference 19 were used to develop graphs of equivalent spherical weights as a function of scaled distance for each azimuth angle and aspect ratio. The side-on pressure and impulse data from Reference 19 for 8-lb Pentolite, free-air cylinders with aspect ratios of 1/4, 1/1, and 4/1 were first adjusted to standard sea-level ambient pressure using Sachs' scaling factors as discussed in Reference 20. The same scaling was also applied to the spherical free-air data recorded throughout the test program described in Reference 19.

Since the experiments were performed with Pentolite charges, the next step in standardizing the data was to convert them to TNT equivalent data. Separate TNT equivalency adjustments were made to the pressure data and to the positive impulse data. TNT equivalency is defined as the ratio of the charge weight of TNT to the weight of the high explosive in question that will yield the same amplitude of a blast parameter at the same radial distance from each charge.

The average pressure or impulse measured on the spherical tests at each of the six scaled distances was used to determine a TNT equivalency for each blast parameter using the standard free-air TNT curve developed by Kingery and Bulmash[3]. The average pressure or impulse at each scaled distance was determined from as many as ten measurements. The equivalency factors at the six scaled distances ranging from about 3 to 15 ft/lb$^{1/3}$ (corrected to sea-level) were then averaged to obtain one value for pressure and one value for impulse which was then applied to the cylindrical data. The average TNT equivalency factor based on the side-on pressure data from the spherical charges was determined to be 1.08. The average TNT equivalency factor based on side-on impulse was 0.9. With these factors, TNT scaled distances for the side-on pressures, and TNT scaled impulses and their corresponding scaled distances were computed from the cylindrical test data already corrected to sea-level conditions.

SPHERICAL EQUIVALENCY FACTORS

With the cylindrical data from Reference 19 scaled to sea-level ambient pressure and in equivalent TNT form, the standard TNT curves were used as the basis for computing spherical equivalency factors. Figure 2 shows one example of a comparison between the side-on pressures from a cylindrical charge of L/D = 4/1 measured at azimuth angles of 22.5°, 45°, 67.5°, and 90° and the spherical TNT curve.

The spherical equivalency factors were determined in a similar way as TNT equivalency weights are generally found. For each cylindrical side-on pressure or impulse data point, an

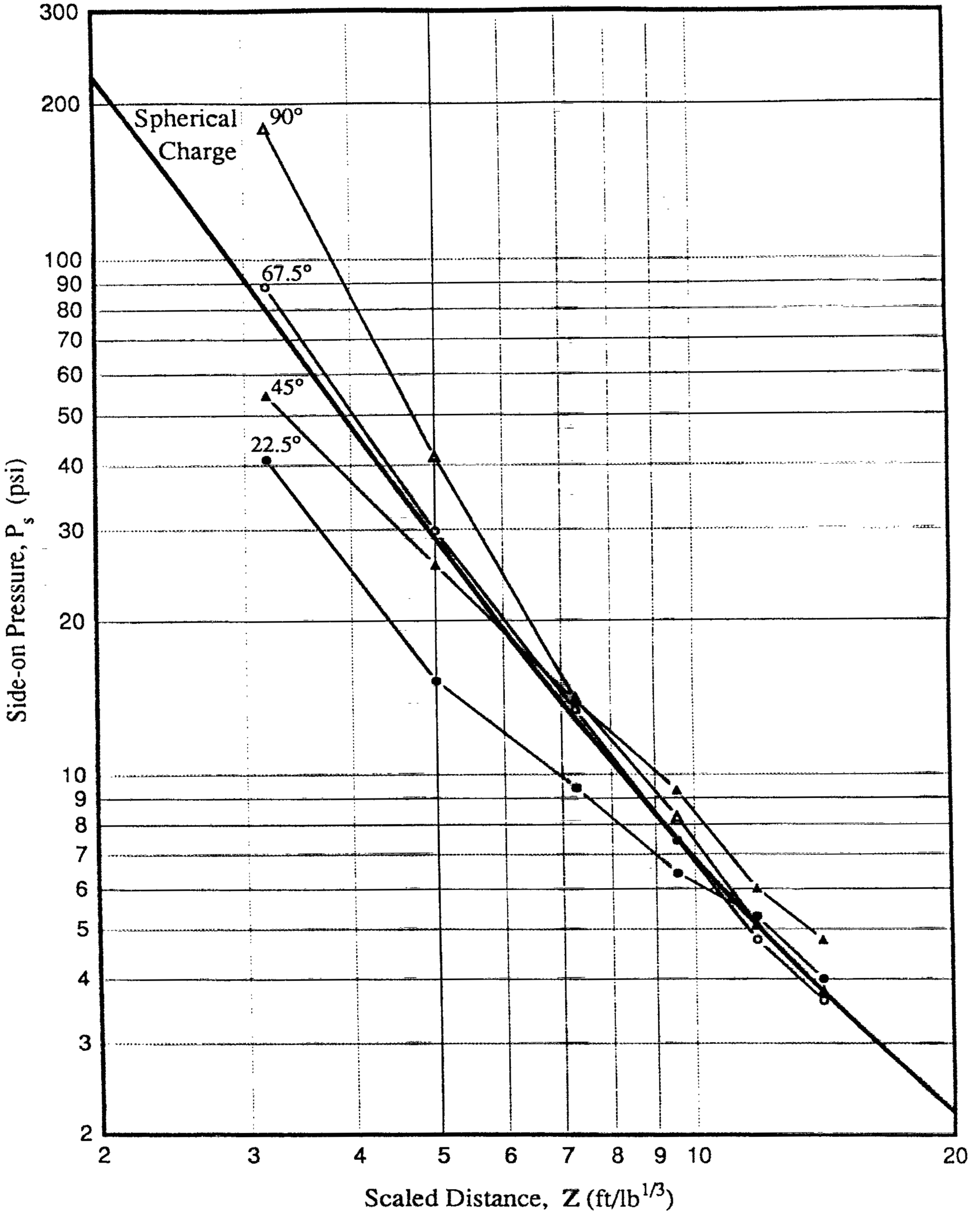

Figure 2. Side-on Pressure Data from a TNT Cylindrical Charge of L/D = 4/1 Compared to TNT Spherical Curve

equivalent spherical weight was determined that would produce the same side-on pressure or impulse at the same distance, R. Thus, for side-on pressure, the ratio of the charge weight of a sphere W_{sph} to that of a cylinder W_{cyl} is

$$\frac{W_{sph}}{W_{cyl}} = \left(\frac{Z_{cyl}}{Z_{sph}}\right)^3_{P_s = \text{constant}} \tag{1}$$

likewise, for side-on impulse

$$\frac{W_{sph}}{W_{cyl}} = \left(\frac{Z_{cyl}}{Z_{sph}}\right)^3_{i_s = \text{constant}} \tag{2}$$

In these equations, Z_{cyl} is the scaled distance $R/W_{cyl}^{1/3}$ and Z_{sph} is the scaled distance $R/W_{sph}^{1/3}$.

Equivalent spherical mass ratios for cylindrical charges with an aspect ratio of 1/4, 1/1, and 4/1 based on side-on pressure measurements at different azimuth angles are presented in Figures 3 through 7. A similar set of ratios based on side-on impulse data are presented in Figures 8 through 12. As mentioned before, the cylindrical charges were initiated at the 180° end (see Figure 1). Consequently, the data is somewhat unsymmetric about the 90° line. For example, Figure 13 shows the pressure-based equivalency factors for a cylinder with L/D = 4/1 at all the azimuth angles. If a cylindrical charge was to be initiated at the longitudinal center, one would expect similar blast load amplitudes at symmetric angles about the 90° radial, such as 0° and 180°, 45° and 135°, etc. Therefore, to apply the end-initiated cylindrical data to a centrally initiated cylinder, the results in Figures 3 through 12 may be used for angles of 0° to 90° and assume the same amplitudes for corresponding angles greater than 90° up to 180°.

BLAST LOADS FROM A CYLINDRICAL CHARGE

In Reference 20, simple examples are used to show how the data presented in Figures 3 through 12 can be used to determine side-on pressures from a cylindrical charge. In one example, the side-on pressures generated by a cylindrical charge of L/D = 1/1 and a TNT equivalent weight of 57.4 lb are estimated at a standoff distance R of 25 ft and azimuth angles θ of 0°, 45° and 90°. Using Figures 3, 4, and 6 to find the equivalent spherical weight at each angle, and the standard TNT free-air curve for a spherical charge in Reference 20 to find the corresponding pressure, the results were as follows:

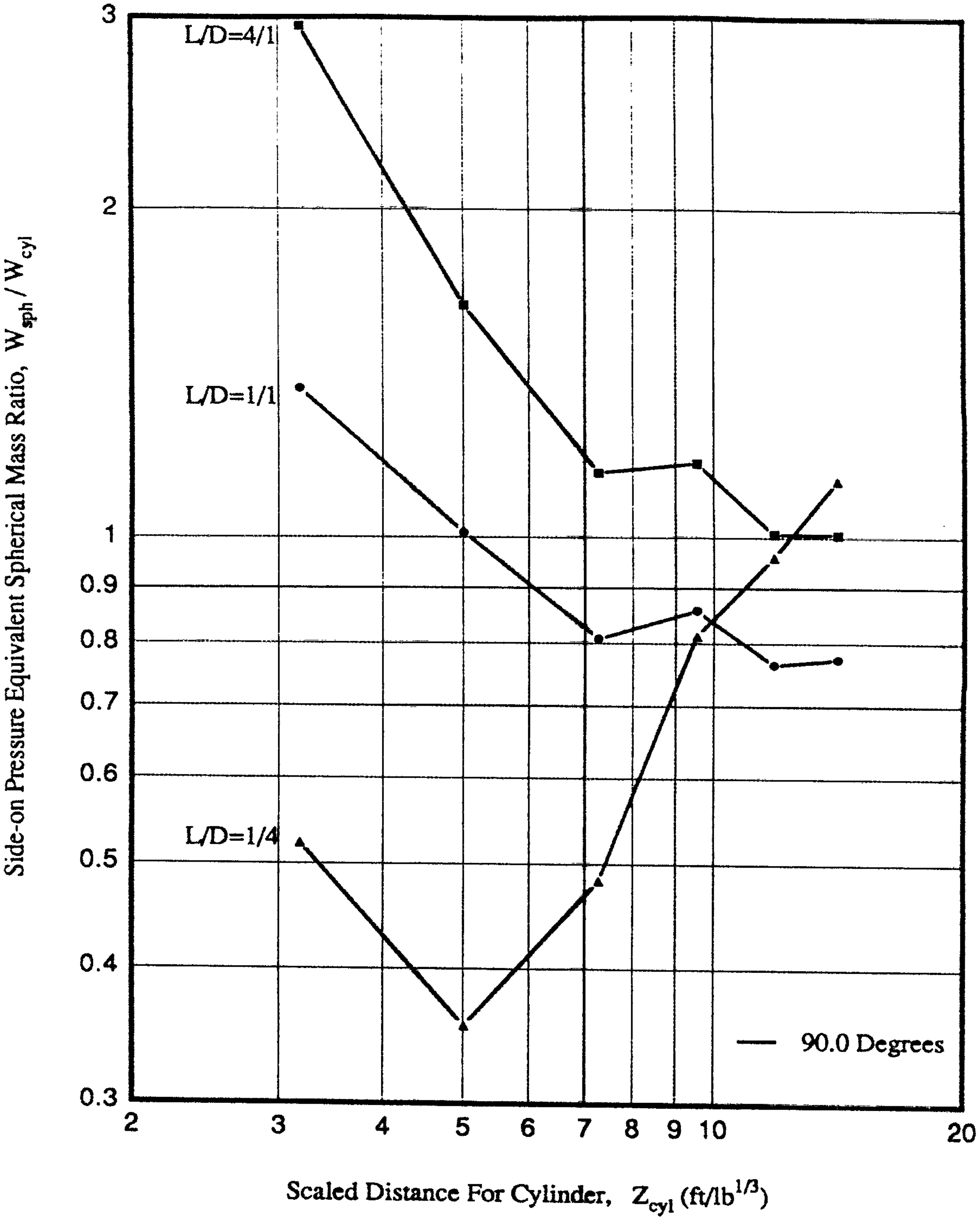

Figure 3. Equivalent Spherical Mass Ratio Based on Experimental Side-on Pressures at an Azimuth Angles of 90° for a Cylindrical TNT Charge Detonated in Free-Air at Sea Level

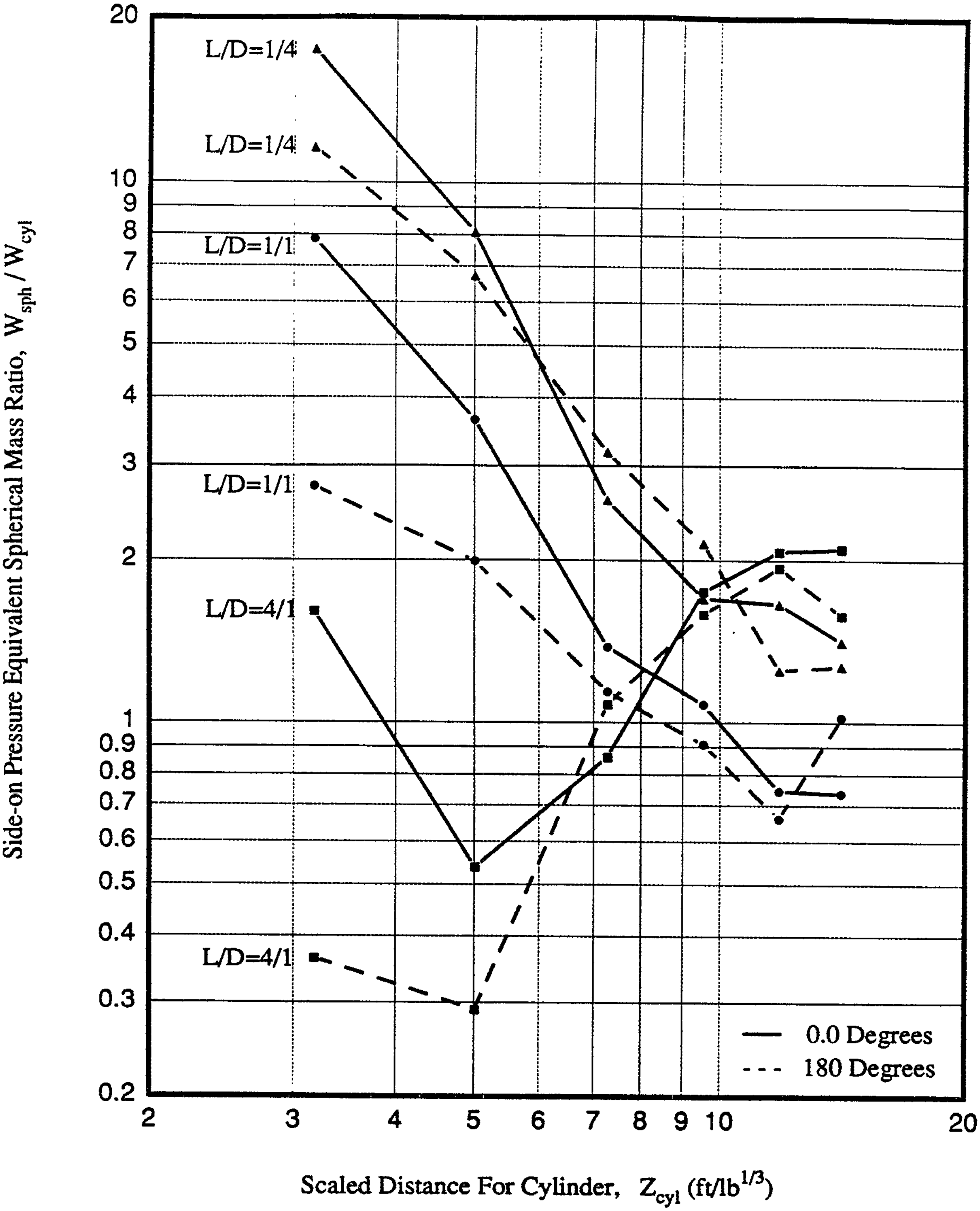

Figure 4. Equivalent Spherical Mass Ratio Bsed on Experimental Side-on Pressures at 0° and 180° for a Cylindrical TNT Charge Detonated in Free-Air at Sea Level

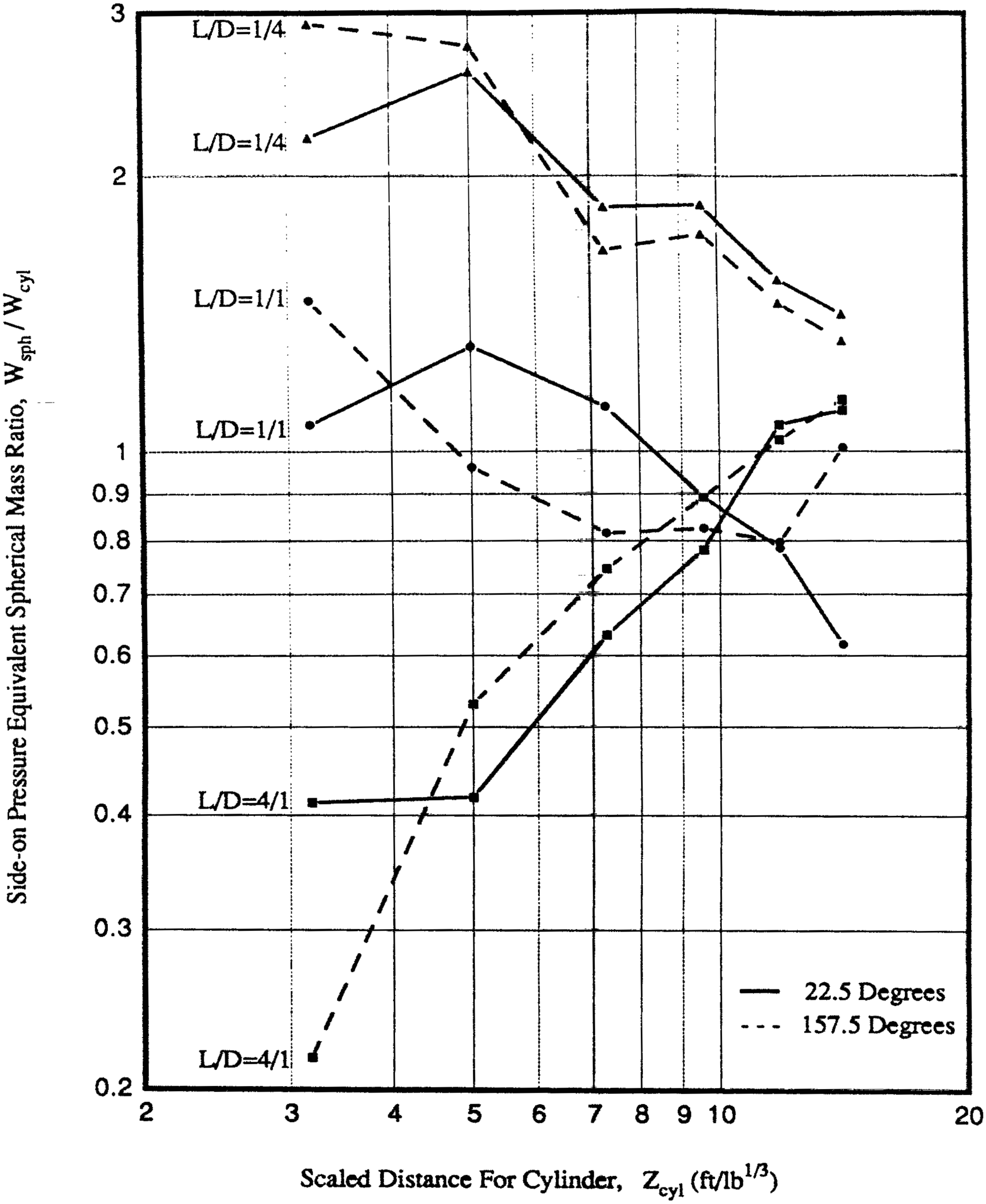

Figure 5. Equivalent Spherical Mass Ratio Based on Experimental Side-on Pressures at 22.5° and 157.5° for a Cylindrical TNT Charge Detonated in Free-Air at Sea Level

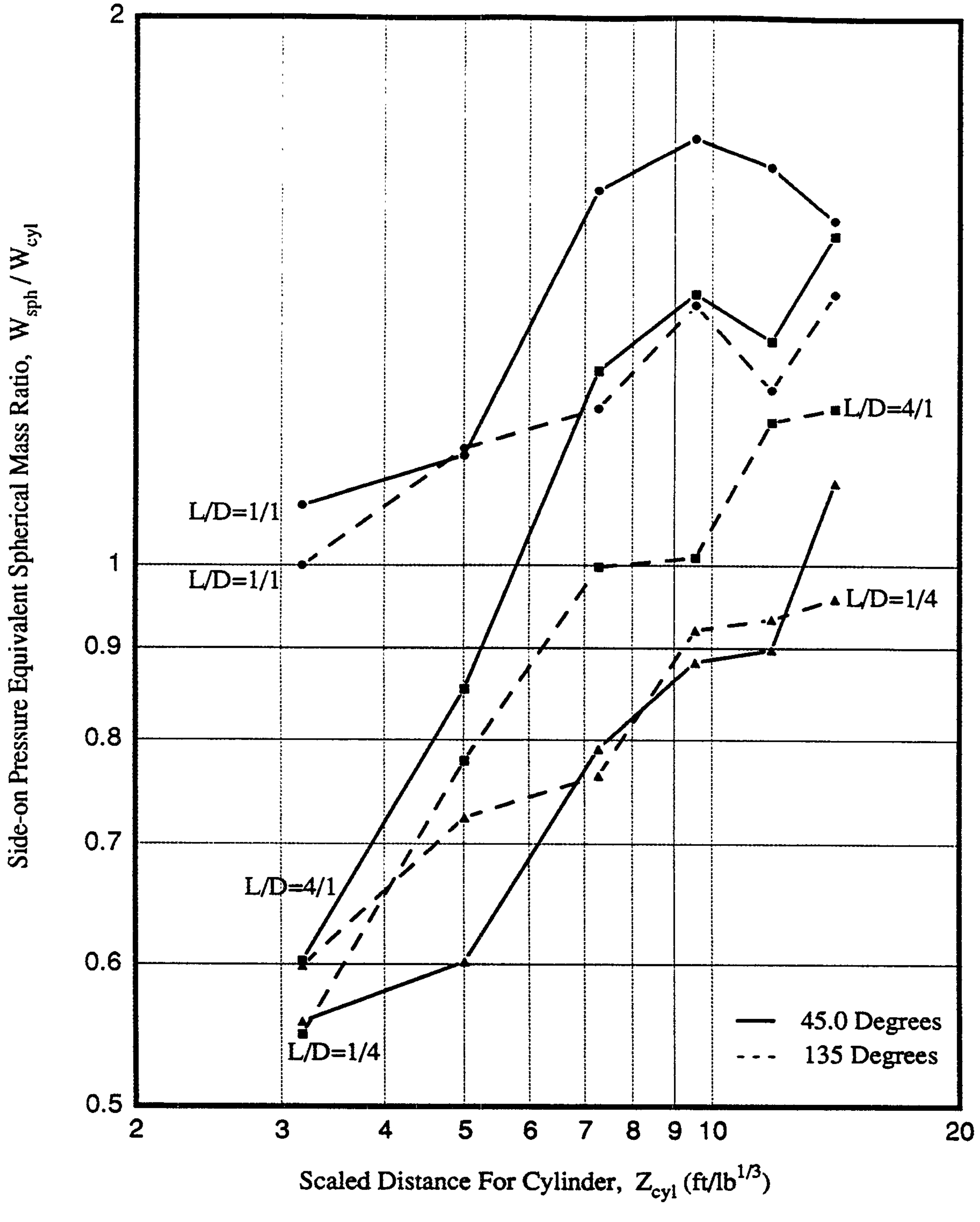

Figure 6. Equivalent Spherical Mass Ratio Based on Experimental Side-on Pressures at 45° and 135° for a Cylindrical TNT Charge Detonated in Free-Air at Sea Level

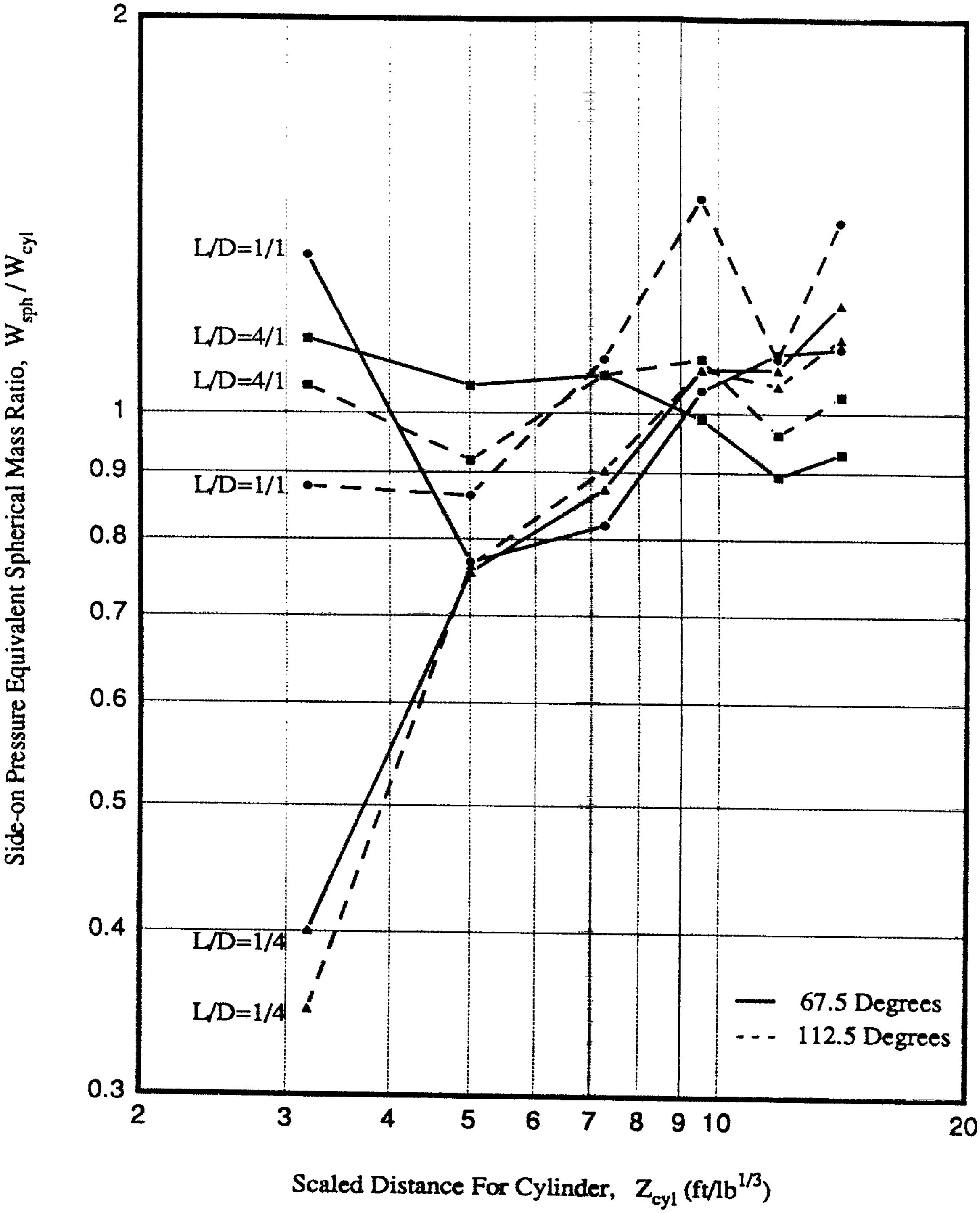

Figure 7. Equivalent Spherical Mass Ratio Based on Experimental Side-on Pressures at 67.5° and 112.5° for a Cylindrical TNT Charge Detonated in Free-Air at Sea Level

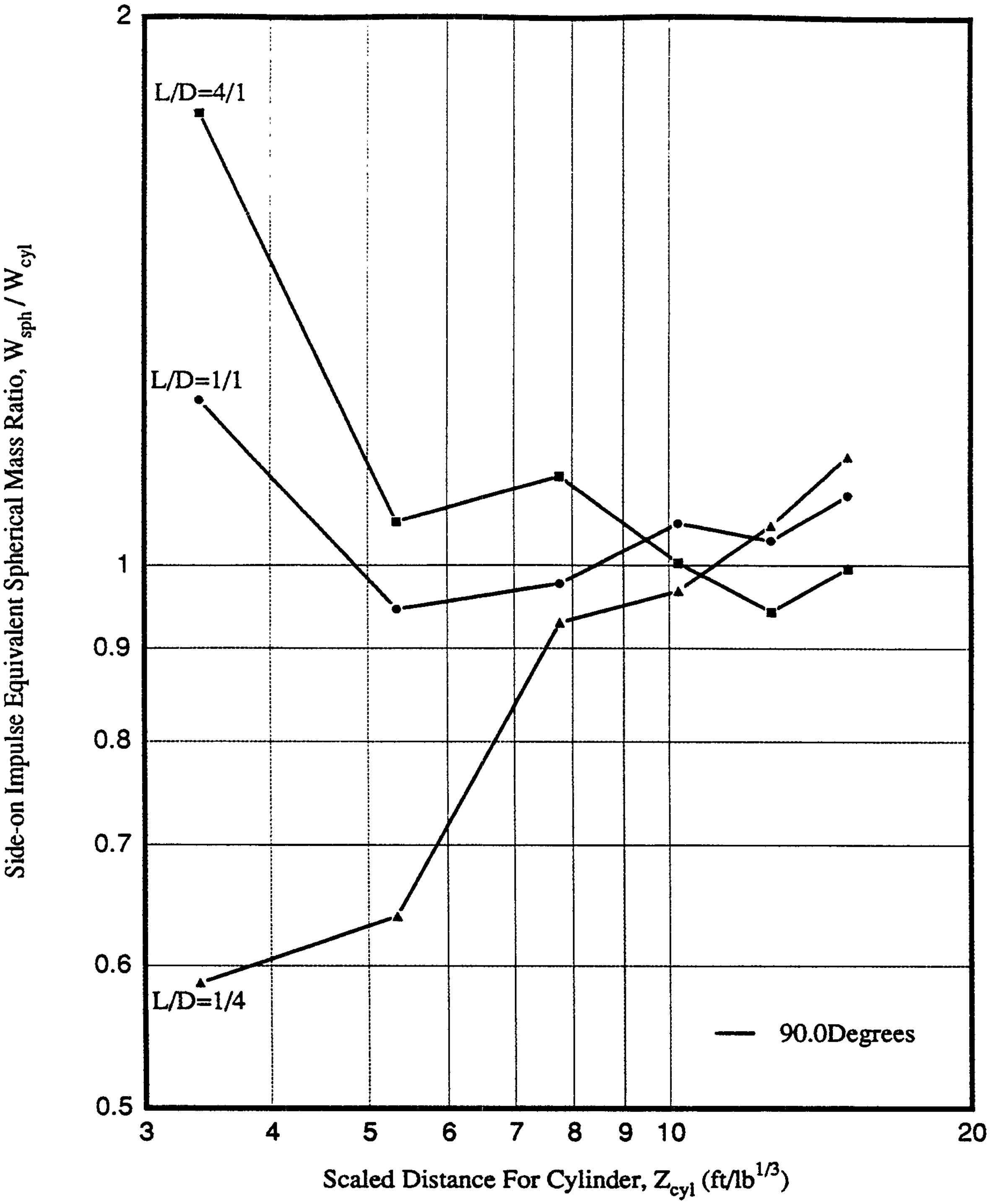

Figure 8. Equivalent Spherical Mass Ratio Based on Experimental Side-on Impulse at an Azimuth Angle of 90° for a Cylindrical TNT Charge Detonated in Free-Air at Sea Level

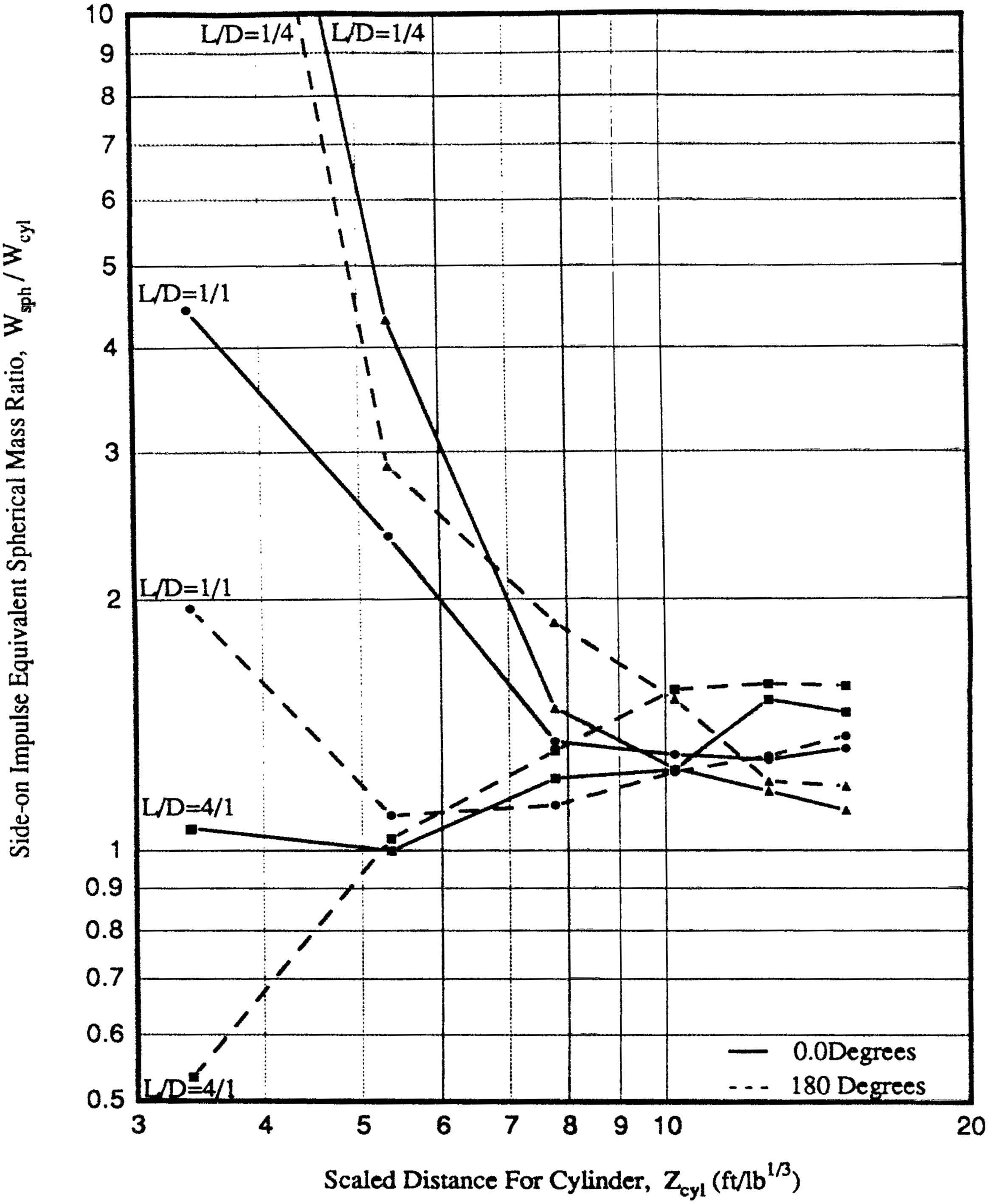

Figure 9. Equivalent Spherical Mass Ratio Based on Experimental Side-on Impulse at 0° and 180° for a Cylindrical TNT Charge Detonated in Free-Air at Sea Level

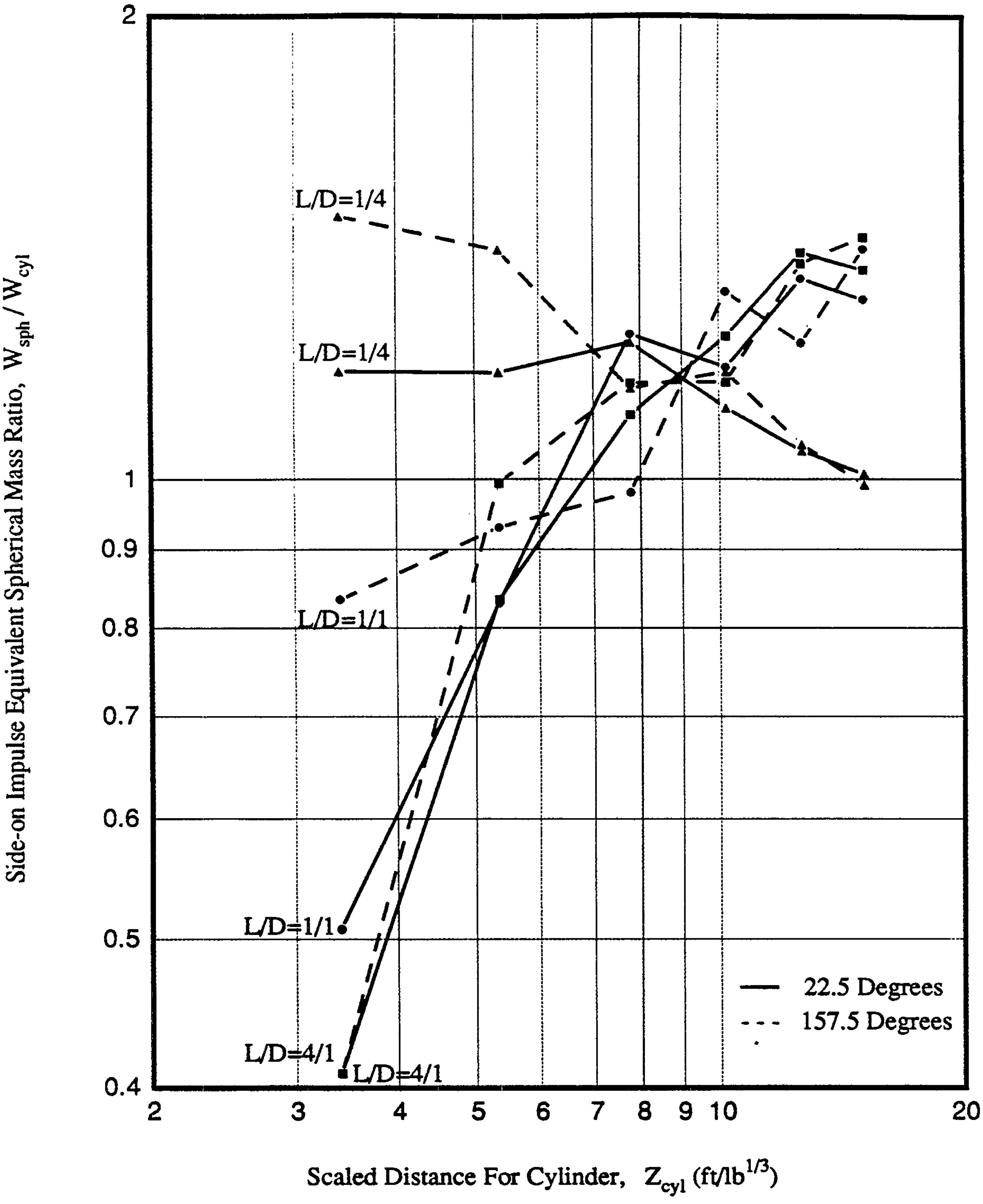

Figure 10. Equivalent Spherical Mass Ratio Based on Experimental Side-on Impulse at 22.5° and 157.5° for a Cylindrical TNT Charge Detonated in Free-Air at Sea Level

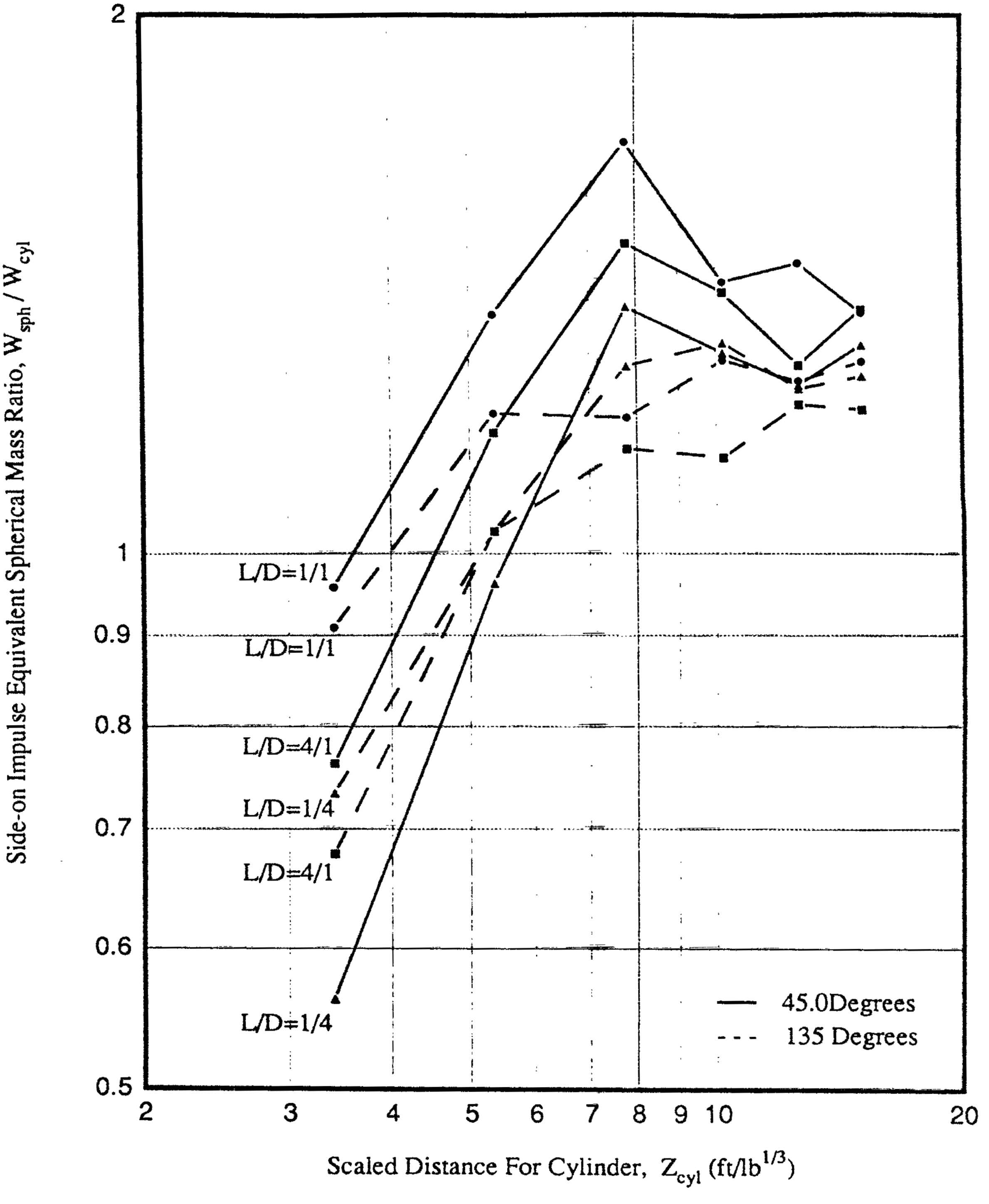

Figure 11. Equivalent Spherical Mass Ratio Based on Experimental Side-on Impulse at 45° and 135° for a Cylindrical TNT Charge Detonated in Free-Air at Sea Level

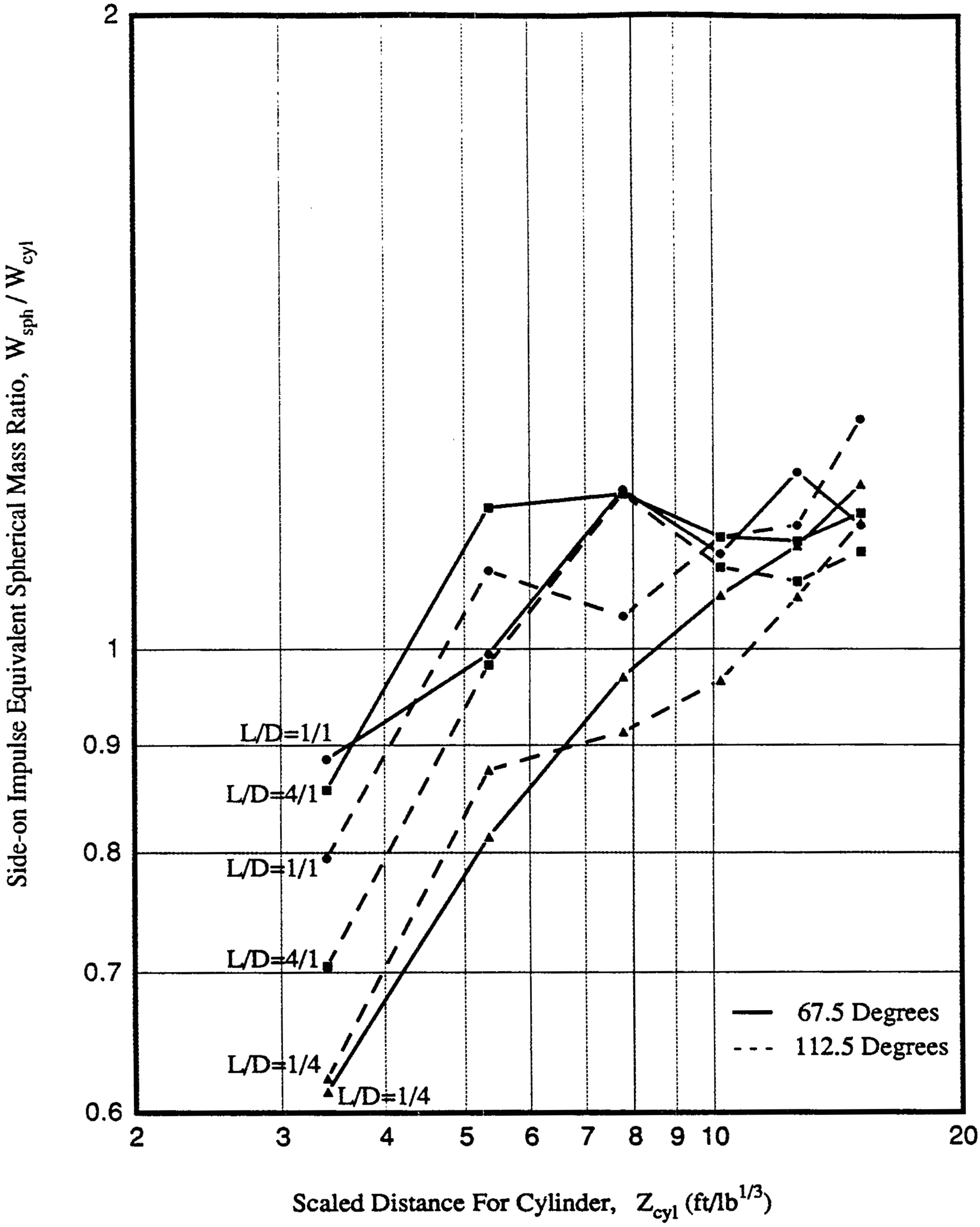

Figure 12. Equivalent Spherical Mass Ratio Based on Experimental Side-on Impulse at 67.5° and 112.5° for a Cylindrical TNT Charge Detonated in Free-Air at Sea Level

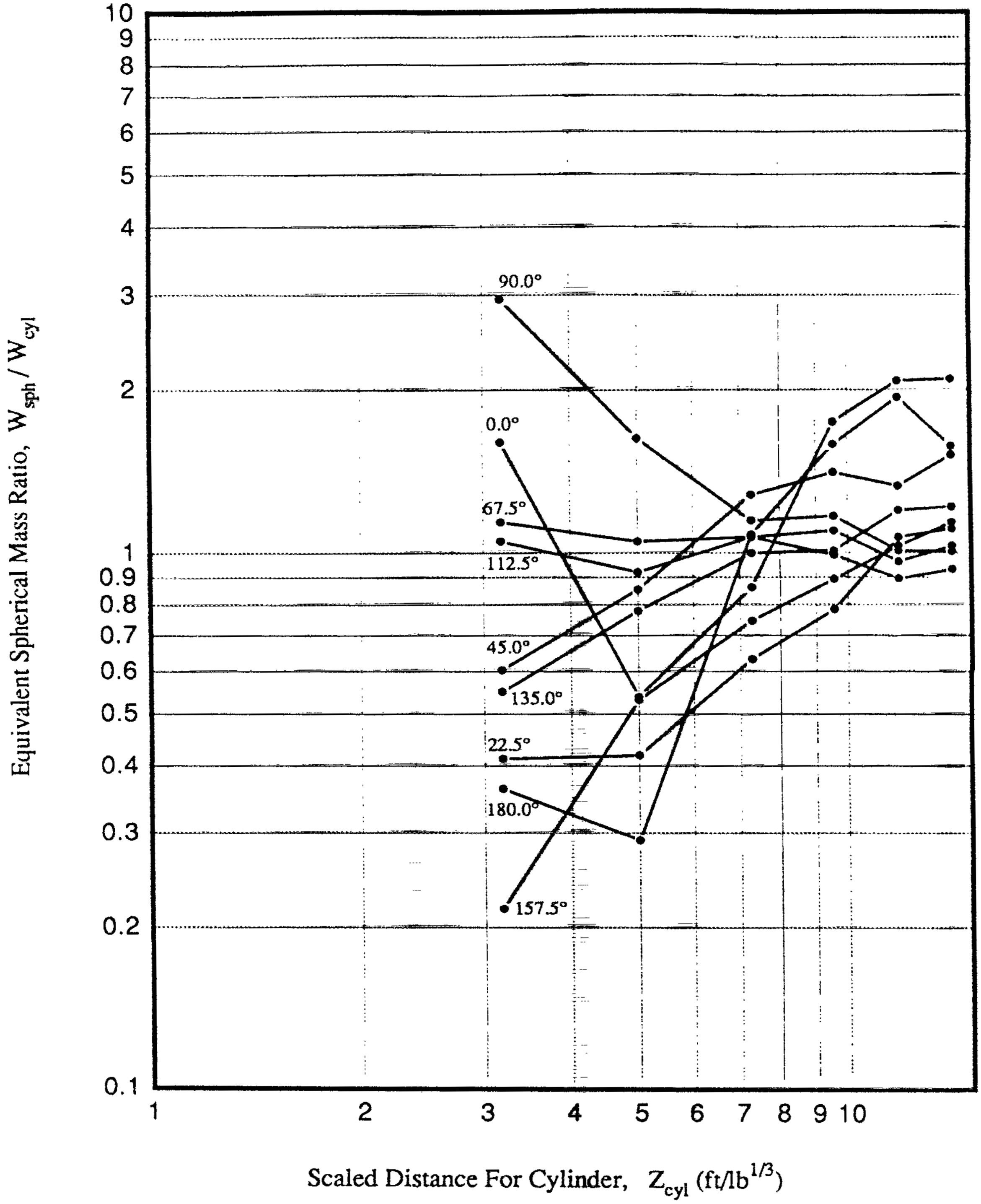

Figure 13. Equivalent Spherical Mass Ratio Based on Side-on Pressure for a Free-Air TNT Cylindrical Charge of L/D = 4/1

W_{cyl} (lb TNT)	R (ft)	$\frac{R}{W_{cyl}^{1/3}}$	θ	$\frac{W_{sph}}{W_{cyl}}$	W_{sph} (lb TNT)	$\frac{R}{W_{sph}^{1/3}}$	P_s (psi)
57.4	25	6.48	0°	1.8	103.3	5.33	25.0
			45°	1.5	86.1	5.66	21.9
			90°	0.86	49.4	6.81	14.7

A spherical charge of the same explosive weight of 57.4 lb at the same standoff distance R of 25 ft would produce a side-on pressure P_s of 16.3 psi. Thus, the difference in the blast pressures produced by the cylindrical charge at that distance can also be presented as ratios of the side-on pressure from the cylindrical charge $P_{s_{cyl}}$ to that from the spherical charge $P_{s_{sph}}$. Therefore, for the above example, the pressure amplitude ratios are:

W_{cyl} (lb TNT)	R (ft)	$\frac{R}{W_{cyl}^{1/3}}$	θ	$P_{s_{cyl}}$ (psi)	$P_{s_{sph}}$ (psi)	$\frac{P_{s_{cyl}}}{P_{s_{sph}}}$
57.4	25	6.48	0°	25.0	16.3	1.53
			45°	21.9	16.3	1.34
			90°	14.7	16.3	0.90

Similar amplitude ratios can be computed using the equivalent spherical mass ratios based on impulse. Note that, in general, the pressure amplitude ratios are quantitatively different from the corresponding spherical mass ratios.

To demonstrate how a cylindrical geometry affects blast loads, amplitude factors as shown above were determined for a cylinder with an L/D = 4/1. A hypothetical problem was devised so that only data from azimuth angles of 22.5° to 90° would be required. Using only the impulse data for the six scaled distances at which measurements were made, amplitude ratios were derived for each of the six scaled distances and smooth curves fitted to extrapolate the data to smaller scaled distances and to interpolate between scaled distances. The results are presented in Figure 14.

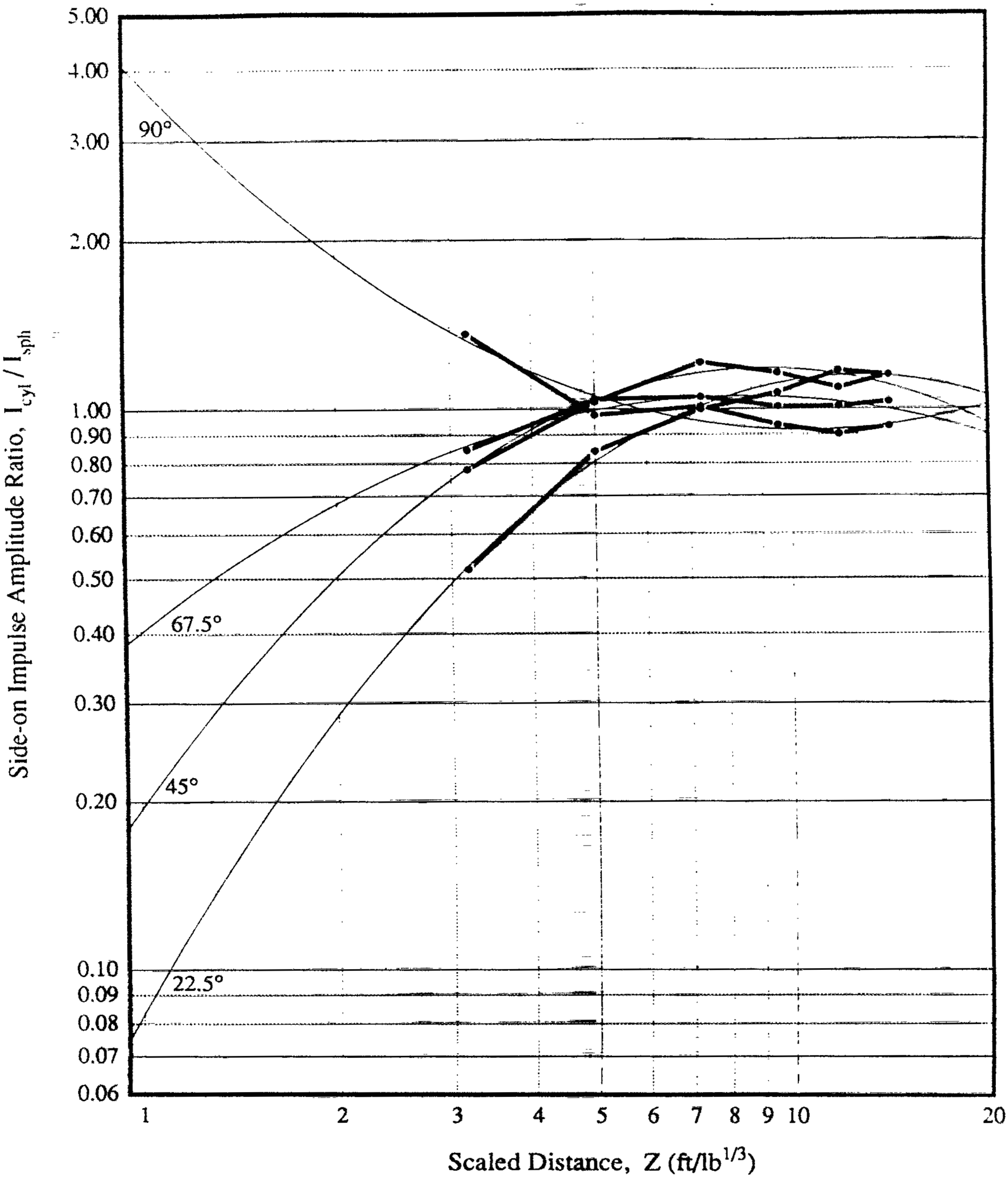

Figure 14. Impulse Amplitude Ratios for a Cylindrical Charge of L/D = 4/1 as Compared to a Spherical Charge

Assuming that reflected impulse will have the same amplitude ratios as side-on impulse, the results presented in Figure 14 were used to estimate the impulsive loads on a flat surface from a free-air cylindrical charge as illustrated in Figure 15. Note that the standoff distance R of 20 ft and the charge weight W of 300 lb were selected such that the cylindrical charge was at a perpendicular scaled distance of 3 ft/lb$^{1/3}$. Thus, very little extrapolation was necessary in using the curves presented in Figure 14. The loads on the flat surface from a spherical charge were first estimated using the computer code CONWEP[21] which has its own set of assumptions. Since the problem is symmetric in two axes, only one quarter of the surface (25 x 15 ft) was used to make the calculations and plot impulse contours as shown in Figure 16. For this case, the average impulse on the quadrant as computed by CONWEP is 210 psi-ms. As expected, the impulse contours are concentric circles. The impulse at the center of each grid element was then adjusted using the curves from Figure 14 for its corresponding azimuth angle and scaled distance. The amplitude ratio curves were interpolated linearly for in between azimuth angles. An impulse contour plot for the cylindrical charge is shown in Figure 17. The contours in this figure are no longer concentric circles and depict quite vividly the effect of the cylindrical charge geometry on the impulse distribution. The average impulse on the quadrant from the cylindrical charge is 325 psi-ms. In a recent limited study by SwRI reported in Reference 22, a similar analysis was used to estimate reflected pressures and impulses on a vertical wall from the detonation of a vertical bomb at the ground surface. In that study, extrapolation of the test data was necessary to a scaled distance of 1.24 ft/1b$^{1/3}$.

CLOSURE

Experimental side-on pressure and impulse data found in the literature from cylindrical charges in free-air were analyzed and used to develop spherical equivalency factors for nine azimuth angles ranging from 0 to 180°. The cylindrical charges of length-to-diameter ratios of 1/4, 1/1, and 4/1 were initiated at the 180° end and measurements made along radial increments of 22.5°. The spherical equivalency factors show the significant difference a cylindrical geometry has on the side-on pressure and impulse, particularly at the smaller scaled distances. These equivalency factors are based on data found in the literature that were measured at scaled distances of about 3 to 15 ft/lb$^{1/3}$. Consequently, the application of this analysis should be limited to scaled distances in this range.

To demonstrate the effect a cylindrical geometry has on blast loads, amplitude factors based on the impulse measurements were computed, extrapolated slightly, and applied in a hypothetical problem to the reflected impulsive loads on a flat surface. In this application it was assumed that

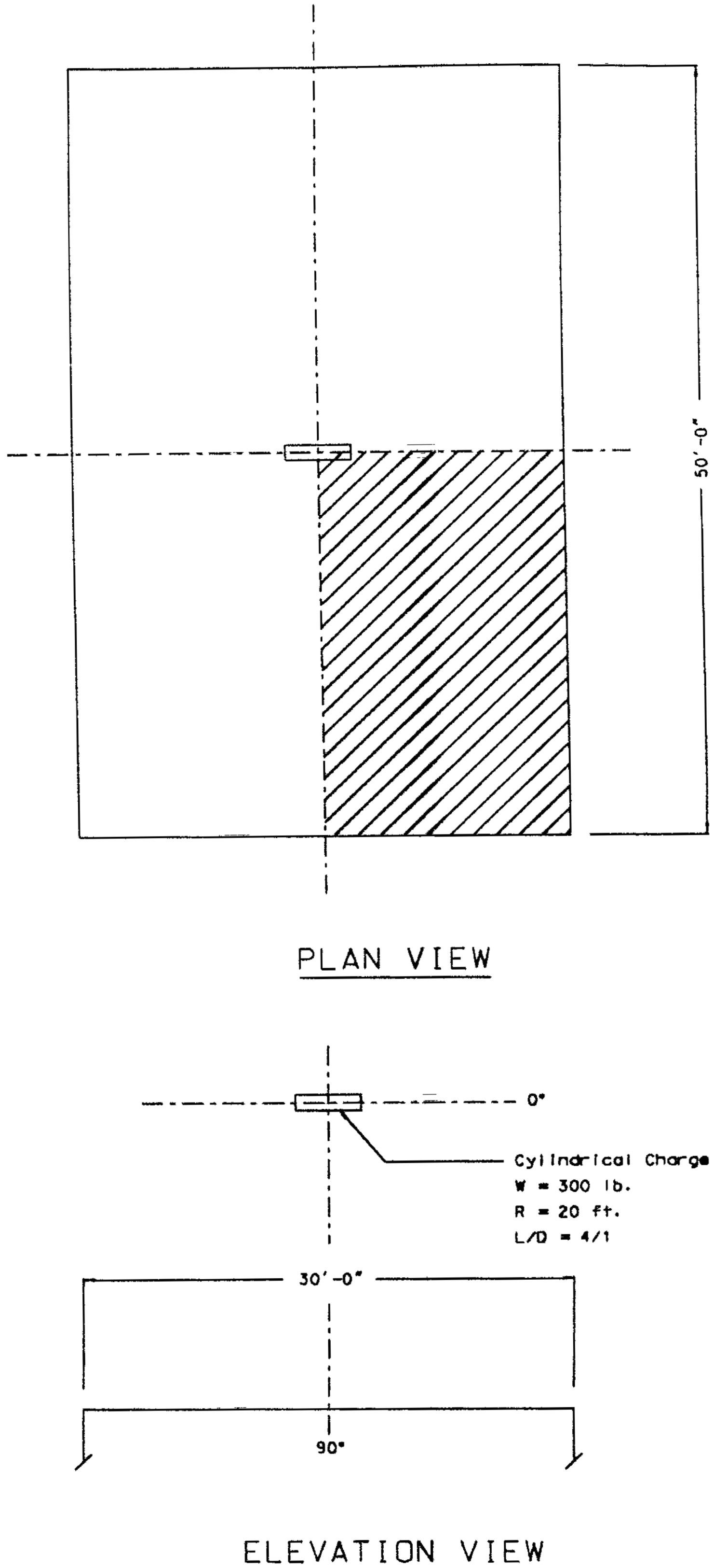

Figure 15. Free-Air Cylindrical Charge Loading a Flat Surface

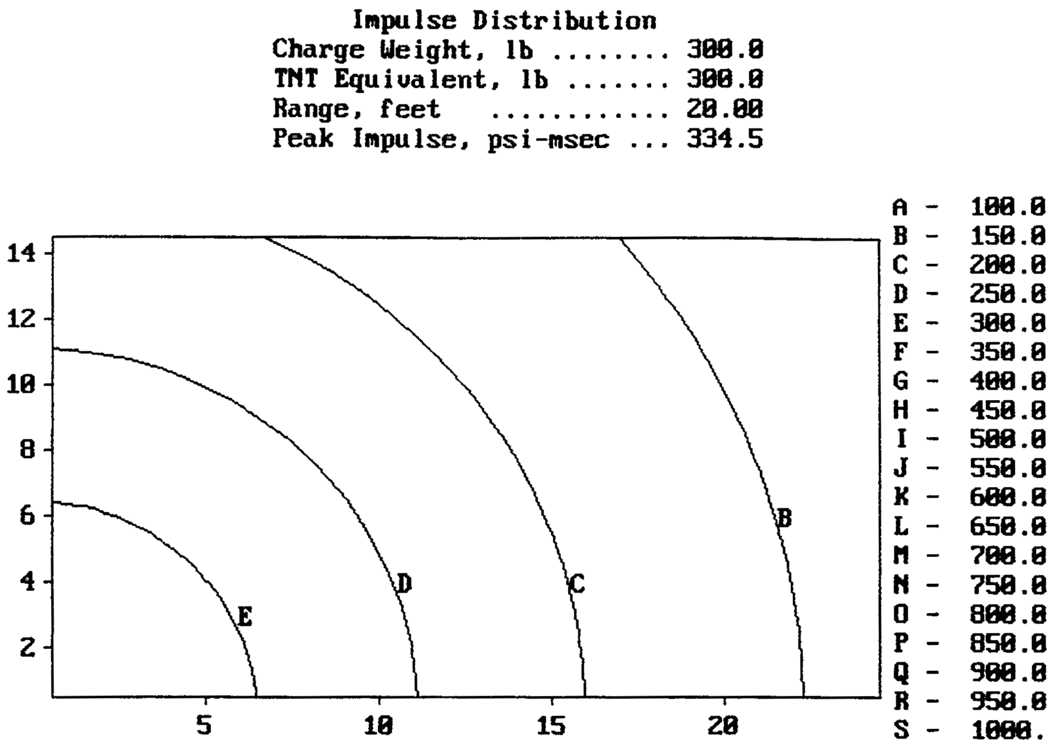

Figure 16. Impulse Contours for a Spherical Charge

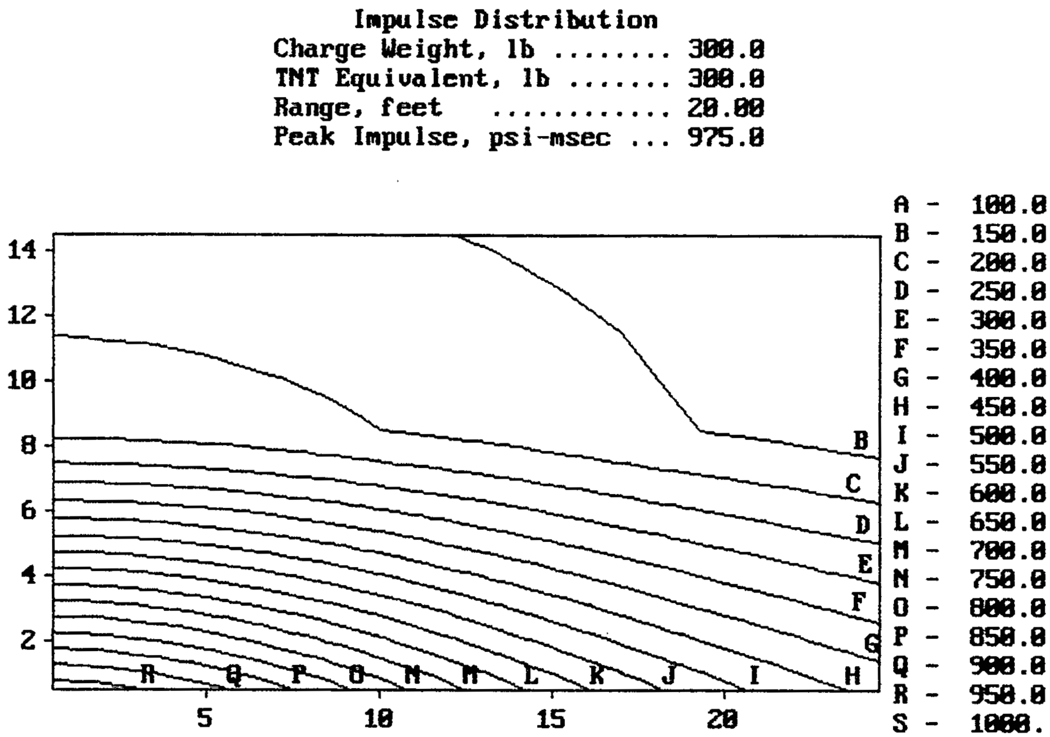

Figure 17. Impulse Contours for a Cylindrical Charge of L/D = 4/1

reflected impulse would have the same amplification factors as side-on impulse. The resulting contour plots depicted quite well the significant difference a cylindrical charge makes on the impulsive loads as compared to a spherical charge.

Considerably more experimental research and data analysis are needed to characterize air blast loads from cylindrical and other nonspherical explosive charges. In particular, measurements of normally and obliquely reflected pressure and impulse are almost nonexistent at small scaled distances where the effects of geometry are most significant. Data are lacking not only from free-air charges, but also from charges on the ground surface. It would be very interesting to determine how close to reality the amplification factors for the illustrated problem really are. The spherical mass ratios presented in this paper provide a means for estimating loads from cylindrical charges of three aspect ratios at scaled distances of about 3 to 15 $ft/1b^{1/3}$. Additional data closer to the charge and with cylinders of other aspect ratios would increase the confidence of the curves presented here.

ACKNOWLEDGEMENTS

Most of the analysis and development of spherical equivalency factors presented in this paper were accomplished as part of the project to revise the U.S. Department of Energy DOE/TIC Manual 11268. Mr. Steve Young of Battelle Pantex was the DOE technical representative and Ms. Patricia Bowles was the SwRI project manager. The author appreciates the resources provided by SwRI to do the additional analysis on amplification factors, and to prepare and present this paper. In particular, the author thanks Mr. Wendell Bielefeld for his significant contribution in the data analysis and curve fits, and for processing most of the figures in this paper. Mr. Jeff Peterson prepared some of the illustrations and Ms. Terry Sloan processed the manuscript.

REFERENCES

1. Goodman, H.J., "Compiled Free Air Blast Data on Bare Spherical Pentolite," BRL Report 1092, Aberdeen Proving Ground, MD, 1960.

2. Baker, W.E., Explosions in Air, University of Texas Press, Austin, Texas, 1973.

3. Kingery, C.N. and Bulmash, G., "Airblast Parameters from TNT Spherical Air Burst and Hemispherical Surface Burst," Technical Report ARBRL-TR-02555, U.S. Army ARDC-BRL, Aberdeen Proving Ground, Maryland, April 1984.

4. Structures to Resist the Effects of Accidental Explosions. Department of the Army Technical Manual TM 5-1300, Department of The Navy Publication NAVFAC P-397, Department of the Air Force Manual AFM 88-22, Department of the Army, the Navy, and the Air Force, June 1969.

5. Structures to Resist the Effects of Accidental Explosions, Department of the Army Technical Manual TM 5-1300, Department of the Navy Publication NAVFAC P-397, Department of the Air Force Manual AFM 88-22, Department of the Army, the Navy, and the Air Force, Revision 1, November 1990.

6. Adams, Channing L., Sarmousakis, James N. and Sperrazza, Joseph, "Comparison of the Blast from Explosive Charge of Different Shapes," Ballistic Research Laboratories, Aberdeen Proving Ground, MD, Report No. 681, January 1949.

7. Makino, R.C. and Goodman H.J., "Air Blast Data on Bare Explosive of Different Shapes and Compositions," BRL Report No. 1015, 1956.

8. Reisler, R.C., "Explosive Yield Criteria," Minutes of 14th Explosives Safety Seminar, New Orleans, 8-10 November 1972, Department of Defense Explosives Safety Board, pp. 271-288.

9. Wenzel, A.B. and Esparza, E.D., "Measurements of Pressures and Impulses at Close Distances from Explosive Charges Buried and in Air," Final Report on Contract No. DAAK 02-71-C-0393 with U.S. Army MERDC, Ft. Belvoir, VA, 1972.

10. Tancreto, J.E., "Effects of Charge Composition and Surface Conditions on Blast Environment," Minutes of the 16th Explosives Safety Seminar, Vol. I, Hollywood, FL, pp. 301-334, September 1974.

11. Reisler, R.E., Giglio-tos, L., and Teel, G.D., "Air Blast Parameters from Pentolite Cylinders Detonated on the Ground," BRL Memorandum Report No. 2471, Aberdeen Proving Ground, MD, 1975.

12. Kulesz, J.J., Esparza, E.D. and Wenzel, A.B., "Blast Measurements at Close Standoff Distances for Various Explosive Geometries," Minutes of the 18th Explosives Safety Seminar, Vol. I, Department of Defense Explosives Safety Board, San Antonio, TX, September 1978.

13. Guerke, G. and Scheklinski-Glueck, G., "Blast Parameters from Cylindrical Charges Detonated on the Surface of the Ground," Minutes of the 20th Explosives Safety Seminar, Vol. I, Norfolk, VA, August 1982.

14. Esparza, E.D., "Reflected Blast Measurements Near Pancake Charges," Minutes of the 24th Explosives Safety Seminar, Vol. I, Department of Defense Explosives Safety Board, St. Louis, MO, August 1990.

15. A Manual for the Prediction of Blast and Fragment Loadings on Structures, U.S. Department of Energy DOE/TIC-11268, November 1980.

16. Plooster, M.N., "Blast Front Pressure From Cylindrical Charges of High Explosives," Naval Weapons Center Technical Memorandum No. 3631, Navy Contract No. N00123-76-C-0166, Denver Research Institute, September 1978.

17. Wisotski, J. and Snyer, W.H., "Characteristics of Blast Waves Obtained from Cylindrical High Explosive Charges," University of Denver, Denver Research Institute, November 1965.

18. Parks, D.K. and Weeding, G.S., "Investigations of Air Blast Parameters Around Cylindrical Charges," University of Denver, Denver Research Institute, January 1959.

19. Plooster, M.N., "Blast Effects from Cylindrical Explosive Charges: Experimental Measurements," Naval Weapons Center Report No. NWC TP 6382, Chia Lake, CA, November 1982.

20. A Manual for the Prediction of Blast and Fragment Loadings on Structures, U.S. Department of Energy DOE/TIC-11268, Revision 1, July 1992.

21. Hyde, D.W., "User's Guide for Microcomputer Programs CONWEP and FUNPRO, Applications of TM5-855-1," Instruction Report SL-88-1, U.S. Army COE Waterways Experiment Station, Vicksburg, MS, April 1988, Revised February 1991.

22. Esparza, E.D., Bielefeld, W.S., and Marchand, K.A., "Reflected Airblast Pressure and Impulse on a Vertical Wall from a Cased Cylindrical Charge Detonated Vertically on the Ground," Southwest Research Institute Letter Report to the U.S.A. Construction Engineering Research Laboratory, Champaign, IL, July 1992.